

Fatigue Properties of Ti-6Al-4V Subjected to Simulated Body Fluid

Y.J. Liu¹, Q.L. Ouyang², R.H. Tian³ and Q.Y. Wang⁴

Abstract: Fatigue properties of Ti-6Al-4V subjected to simulated body fluid (SBF) environment were presented in this paper. Using the ultrasonic fatigue testing technique, the ultra-high cycle fatigue properties of Ti-6Al-4V alloy subjected to SBF in two groups for two days and six days respectively in body temperature were studied and the initiation mechanisms of fatigue cracks were investigated and analyzed with scanning electron microscopy (SEM) and energy dispersive atomic X-ray (EDX). Then, a comparison with corresponding behaviors of the Ti-6Al-4V alloy with no treatment was made. The results show that, the S-N curves of the Ti-6Al-4V alloy after subjection have the similar tendency with that with no treatment, that is, they descend continuously during 10^4 and 10^8 cycles and the descending tendency is lower in the region of 10^7 - 10^8 cycles; the life of the specimens after subjection descends heavier before the fatigue life of 10^7 cycles and is lower after the fatigue life of 10^7 cycles than that with no treatment; the life of the specimens subjected for six days has little difference with that subjected for two days. Fatigue failure initiates from internal inclusion where mostly the element Al aggregates at the ultra-high cycle regime.

Keywords: Ti-6Al-4V, Ultrasonic fatigue, S-N curve, Crack initiation, Simulated body fluid

1 Introduction

The Ti-6Al-4V alloy exhibits an excellent combination of properties, including high specific strength and stiffness, outstanding corrosion resistance and excellent biocompatibility, which provide a great potential for biomedical applications. Therefore, titanium and its alloy are nearly ideal implant materials for the development of medical bone reinforcement and replacement products [Ferri, Ebel and

¹ Department of Mechanics and Engineering Science, Sichuan University, Chengdu, China

² Luoyang LYC Bearing Co. Ltd, Luoyang, China

³ Department of Mechanics and Engineering Science, Sichuan University, Chengdu, China

⁴ Department of Mechanics and Engineering Science, Sichuan University, Chengdu, China

Bormann (2009)]. At present, the Ti-6Al-4V is one of the bio-engineering materials in common use [Feng, Kang and Zhang(2001); Yu and Zhang(2000)].

Although titanium based alloys exhibit good corrosion resistance due to the formation of its surface, the nature, composition and thickness of the protective oxide scales depend on environmental conditions. The fatigue crack propagation resistance of Ti-6Al-4V under aqueous saline environments and medical alcohol has been reported, which is insensitive [Cao, Murakami and Wang (2010)]. Implants usually bear alternating load of low stress at a long time. For example, artificial joint may bear impact and fretting loads which are times more than avoirdupois for about 3.6×10^6 cycles each year. Consequently, to predict service life of the Ti-6Al-4V implant, it is valuable to study its ultra-high cycle fatigue behaviors in physiological environment.

The paper deals with the fatigue properties of Ti-6Al-4V subjected to simulated body fluid (SBF) environment, up to very high cycles. For comparing, the specimens have been dipped into SBF in two groups for two days and six days respectively at 37° prior to fatigue test.

2 Experiment

2.1 Material

The chemical composition and mechanical properties of the Ti-6Al-4V alloy are presented in Table 1 and Table 2 respectively.

Table 1: The chemical composition [wt%]

Ti	Al	V	Fe	Si	C	N	H	O
rest	5.5~6.8	3.5~4.5	0.30	0.15	0.10	0.05	0.015	0.20

Table 2: The mechanical properties

E /GPa	σ_s /MPa	σ_b /MPa	ρ /g.cm ⁻³	A%
106	891	1009	4440	10

2.2 Fatigue Testing

The dimensions of the specimen need to be determined for the demands that the inherent frequency of first step mode of longitudinal vibration of the specimen have to be equal to the frequency of the ultrasonic fatigue testing system. The testing

specimen has a shape of hourglass variable section with catenary in the middle and cylinder at both ends as shown in Figure 1. The detailed dimensions of the specimens are listed in Table 3. R_1 and R_2 are the radii of circular sections at the location of the middle and the end, respectively. L_1 and L_2 are the lengths of the catenary and resonance of the specimen, respectively.

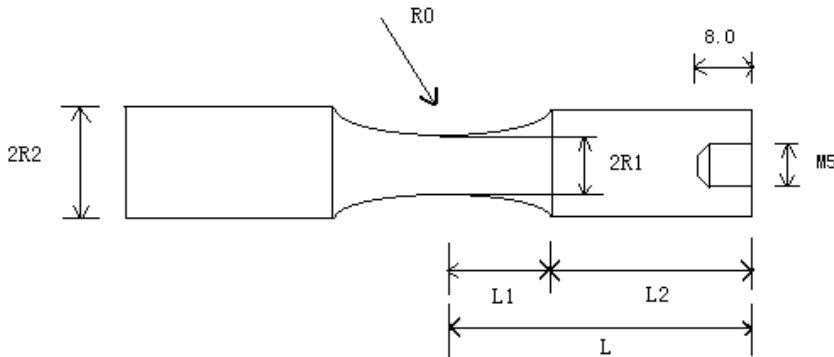


Figure 1: Geometrical characteristics of specimen

Table 3: Physical dimensions (mm)

R_1	R_2	R_0	L_1	L_2
1.5	5.0	31	14.3	16.1

Tests were performed using a setup of USF-2000 made in JAPAN under axial cyclic loads with stress ratio of $R = -1$ [Wang, Ning, Yuan and Yan (2002); Wang (2002); Wang, Bathias, Kawagoishi and Chen(2002)]. The standard resonance frequency of the system is 20KHz. Compressive condensing air was used as the cooling medium. In order to reduce the increase of temperature caused by absorbing energy of ultrasonic vibration and internal frictional heat, the interval loading method was adopted, that is, 300 msec working time with an interval time of 200 msec.

2.3 Dipping Testing

The SBF was made according to the process proposed by Kokubo and Takadama (2006). The comparison of the ion concentration of SBF and human body plasma is presented in Table 4. Two groups of specimens have been dipped into SBF at 37°C for 2 days and 6 days respectively prior to fatigue test.

Table 4: Ion concentrations of SBF and human blood plasma (Mmol/L)

	Na ⁺	K ⁺	Ca ²⁺	Mg ²⁺	HCO ³⁻	Cl ⁻	HPO ⁴ ³⁻	SO ⁴ ²⁻
human blood plasma	142.0	5.0	2.5	1.5	27.0	103.0	1.0	0.5
SBF	142.0	5.0	2.5	1.5	4.2	148.5	1.0	0.5

2.4 Fractography

The fracture surfaces of specimens were investigated by SEM (Scanning Electron Microscope) in order to capture information on the fatigue crack initiation and propagation mechanisms involved, particularly at ultra-high cycles.

3 Results and Discussion

3.1 S-N Diagram

Results from fatigue tests performed on the three groups of specimens are shown by means of the S-N data in Figure 2. It is evident that fatigue failure occurs up to the ultra-high cycle regime although the variation is gradual. Specimens that did not encounter failure are shown with arrows. It is clearly seen that fatigue failure occurs beyond 10^7 cycles and right up to the ultra-high cycle regime, without the presence of an endurance limit in the vicinity of a million cycles. The S-N curves of the Ti-6Al-4V alloy after subjection has the similar tendency with that of the untreated one, that is, they descend continuously during 10^4 and 10^8 cycles and the descending tendency is lower in the region of 10^7 - 10^8 cycles. Furthermore, the life of the specimens after subjection is lower after the fatigue life of 10^7 cycles than that with no treatment and the life of the specimens subjected for six days has little difference with that subjected for two days. The logarithmic linear fitting has been marked in the diagram. It shows that the life of the specimens after subjection descends heavier before the fatigue life of 10^7 cycles than that with no treatment. Logarithmic linear fitting expressions are listed in (1)-(3).

$$\text{No treatment: } S = -4.829 \ln(N) + 765.25 \quad (1)$$

$$\text{Dipped for 2 days: } S = -8.9773 \ln(N) + 826.09 \quad (2)$$

$$\text{Dipped for 6 days: } S = -7.1744 \ln(N) + 802.11 \quad (3)$$

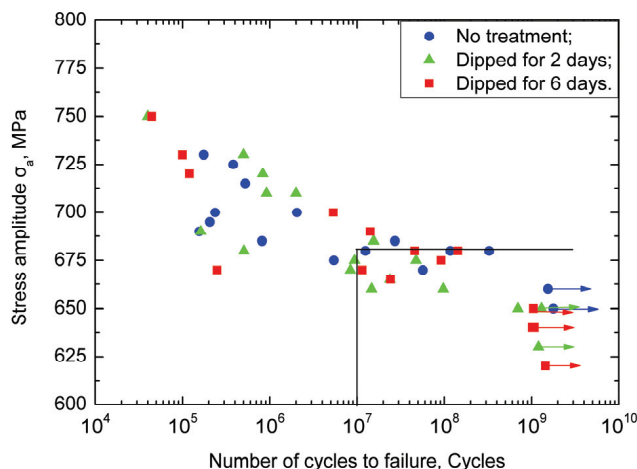


Figure 2: S-N diagram

3.2 Fracture Characteristics

Preliminary SEM observations on the ultra-high cycle fatigue fracture in Ti-6Al-4V reveal subsurface crack initiation resulting in a fish-eye fracture. The fracture surfaces of the Ti-6Al-4V that failed in about 10^8 cycles are shown in Figure 3, Figure 4 and Figure 5 for the cases of untreated, dipped for 2 days and dipped for 6 days specimens, respectively. It is seen that the crack has initiated at an inclusion located beneath the specimen surface. More detailed fractographies of the crack initiation areas are obtained as shown in Figure 3(b)(c), Figure 4(b) and Figure 5(b), respectively. The EDX analyses of these inclusions are shown in Figure 3(d) and Figure 4(c). Obviously, there is the apex of the element Al. The crack has then grown radially outward and propagated rapidly leading to a catastrophic failure. The optically dark area (ODA) around the inclusion, typically seen in a fish-eye fracture, is also clearly noticed here. Fatigue striation and dimple are evident in the fracture surface. Therefore, ultrasonic fatigue fracture of Ti-6Al-4V is transcrystalline plastic.

4 Conclusions

The experimental results indicate that fatigue failure occurs in the ultra-high cycle regime. The results show that the S-N curve of the Ti-6Al-4V alloy after subjection has the similar tendency with that of the untreated one, that is, they descend

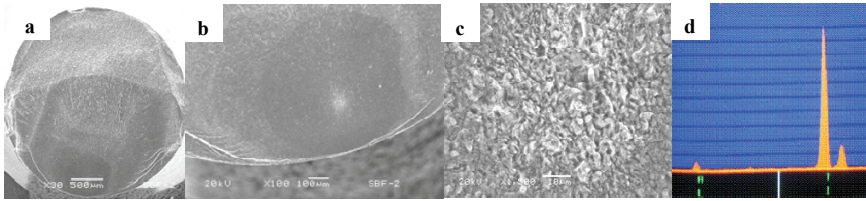


Figure 3: Characteristics of fracture surface ($\sigma_{\max} = 680\text{MPa}$, $N_f = 1.17 \times 10^8\text{Cycles}$, no treatment); a—overall view of fracture surface; b—Crack initiation area at high magnification (100 times); c—Crack initiation area at high magnification (1500 times); d—Energy dispersive atomic X-ray result.

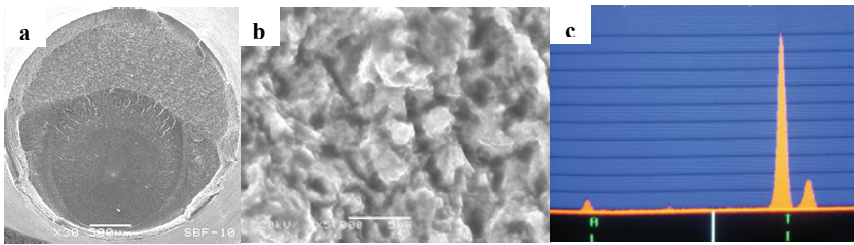


Figure 4: Characteristics of fracture surface ($\sigma_{\max} = 650\text{MPa}$, $N_f = 6.97 \times 10^8\text{Cycles}$, dipped for 3 days); a—overall view of fracture surface; b—Crack initiation area at high magnification; c—Energy dispersive atomic X-ray result.

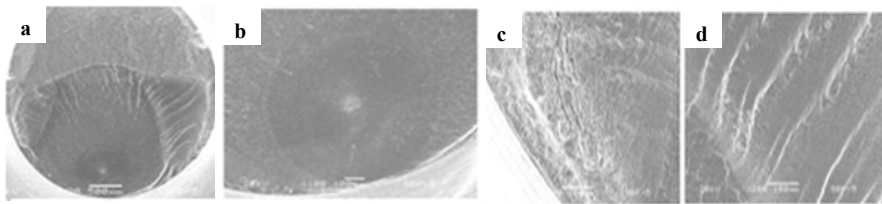


Figure 5: Characteristics of fracture surface ($\sigma_{\max} = 680\text{MPa}$, $N_f = 1.43 \times 10^8\text{cycles}$, dipped for 6 days); a—overall view of fracture surface; b—Crack initiation area at high magnification; c&d—Fatigue striation.

continuously during 10^4 and 10^8 cycles and the descending tendency is lower in the region of 10^7 - 10^8 cycles. The life of the specimens after subjection descends heavier before the fatigue life of 10^7 cycles and is lower after the fatigue life of 10^7 cycles than that with no treatment, which indicates the ultra-high cycle fatigue

property of the Ti-6Al-4V alloy is a little decreased after SBF subjection. The life of the specimens subjected for 6 days has little difference with that subjected for 2 days. Fracture can still occur beyond 10^7 cycles showing there is no fatigue limit as the traditional fatigue conception describes. Fatigue cracks mainly initiate from surface of specimen before the fatigue life of 10^7 cycles. Fatigue failure initiates from internal inclusion where mostly the element Al aggregates after the fatigue life of 10^8 cycles. The fracture surfaces are generally rough and exhibit transcrystalline features.

Acknowledgement: The financial support extended by the China National Funds for Distinguished Young Scientists (10925211) and the National Science Foundation of China (NSFC-50878174) are gratefully acknowledged.

References

Cao, X. J.; Murakami, R. I.; Wang, Q. Y. (2010): Fatigue Properties of Ti-6Al-4V Subjected to 0.9% Physiological Saline Solution. *International Journal of Modern Physics B*, vol. 24, no. 15-16, pp. 2518-2523.

Feng, Y. F.; Kang, H. F.; Zhang, Z. (2001): Progress in Research and Application of Ti alloy for Medical Implants. *Chinese Journal of Rare Metals*, vol. 9, pp. 349-354.

Ferri, O. M.; Ebel, T.; Bormann, R. (2009): High cycle fatigue behaviour of Ti-6Al-4V fabricated by metal injection moulding technology. *Materials Science and Engineering A*, vol. 504, pp. 107-113.

Kokubo, T.; Takadama, H. (2006): How useful is SBF in predicting in vivo bone bioactivity. *Biomaterials*, vol. 27, no. 15, pp. 2907 - 2915.

Wang, Q. Y.; Ning, J. X.; Yuan, X. M.; Yan, H. Q. (2002): Thermo-ultrasonic Fatigue Behavior for Nodular Cast Iron in Super-long Life Range. *Journal of Experimental Mechanics*, vol. 17, no. 4, pp. 483-487.

Wang, Q. Y. (2002): Accelerated Fatigue Testing by Ultrasonic loading. *Journal of Sichuan University (Engineering Science Edition)*, vol. 34, no. 3, pp. 6-11.

Wang, Q. Y.; Bathias, C.; Kawagoishi, N.; Chen, Q. (2002): Effect of inclusion on subsurface crack initiation and gigacycle fatigue strength. *International Journal of Fatigue*, vol. 24, pp. 1269-1274.

Yu, Y. T.; Zhang, X. D. (2000): *Bio-medical Materials*. Tianjin Univ. Press.

